Available online at www.sciencedirect.com

ScienceDirect

JOURNAL OF IRON AND STEEL RESEARCH, INTERNATIONAL. 2016, 23(10): 1119-1126

Wear Behavior of Aluminum Matrix Hybrid Composites Fabricated through Friction Stir Welding Process

Halil Ibrahim KURT[1], Murat ODUNCUOGLU[1], Ramazan ASMATULU[2]

(1. Department of Mechanical and Metal Technologies, Technical Sciences, Gaziantep University, Gaziantep 27310, Gaziantep, Turkey; 2. Department of Mechanical Engineering, Wichita State University, Wichita 67260, KS, USA)

Abstract: Effects of friction stir processing (FSP) parameters and reinforcements on the wear behavior of 6061-T6 based hybrid composites were investigated. A mathematical formulation was derived to calculate the wear volume loss of the composites. The experimental results were contrasted with the results of the proposed model. The influences of sliding distance, tool traverse and rotational speeds, as well as graphite (Gr) and titanium carbide (TiC) volume fractions on the wear volume loss of the composites were also investigated using the prepared formulation. The results demonstrated that the wear volume loss of the composites significantly increased with increasing sliding distance, tool traverse speed, and rotational speed; while the wear volume loss decreased with increasing volume fraction of the reinforcements. A minimum wear volume loss for the hybrid composites with complex reinforcements was specified at the inclusion ratio of 50% TiC+50% Al_2O_3 because of improved lubricant ability, as well as resistance to brittleness and wear. New possibilities to develop wear-resistant aluminum-based composites for different industrial applications were proposed.

Key words: aluminum alloy; friction stir processing; wear; hybrid composite; modeling

Metal matrix composites (MMCs) are widely used in aerospace, automobile, military, and biomedical applications because of their high specific strength and considerably low density. In the fabrication of MMCs, aluminum (Al) is one of the most popular matrix materials because of its low density, good corrosion resistance and strengthening capability[1-5]. Aluminum matrix composites (AMCs) are utilized in a wide range of components for advanced manufacturing. It was reported that fuel consumption, pollution, and overall weight in aircraft and automobiles can be reduced by using AMCs in many engine block and frame applications[6,7].

AMCs can be reinforced by ceramic particles such as SiC, SiO_2, Al_2O_3, BN, B_4C, WC, TiC, and AlN, or whiskers and fibers of various types. Among these ceramics, SiC and Al_2O_3 are widely employed in tribological applications because they provide superior hardness for improving the wear resistance of final products[8-12].

AMCs can be fabricated by casting, powder metallurgy, sintering, friction stir processing (FSP), and spray co-deposition methods[13-16]. FSP method is based on friction stir welding and was explained in Refs. [17-20] in detail. The most important FSP parameters are shoulder dimension, pin shape and dimension, tilt angle, tool rotational speed and traverse speed, and the number of passes[21]. The distribution of particles can be improved by rising the rotational speed and decreasing the travel speed, but the increase in tool travel speed may lead to a lower heat input and premature microstructures in the heat-affected and thermo-mechanical-affected zones[22].

Mahmoud et al.[23] investigated the effect of the tool pin profile on the distribution of particles, and reported that SiC particles were distributed more homogeneously in Al using a square probe tool instead of circular or triangle probe tools. Al/TiB_2 composites were fabricated by using square and hexagon pin geometry, and the best mechanical properties were obtained by using a straight square tool pin profile, which contributed to the uniform distribution of TiB_2[24]. A356 and AA6061 alloys were welded using various pin shapes with different tool

Biography: Halil Ibrahim KURT, Doctor, Associate Professor; **E-mail**: hiakurt@gmail.com; **Received Date**: November 9, 2015

shoulder diameters. It was reported that under the same experimental condition, higher tensile strength was obtained with the hexagonal pin with a shoulder diameter of 15 mm[25]. MMCs can be processed by one or more passes and different tilt angles. Besides, the effects of pass numbers and tilt angles on the mechanical properties of composites were clearly emphasized in Refs. [26-28].

It is well known that the tensile and wear properties of composites fabricated by friction stir processing method are affected by a number of factors like the tool/pin geometry, processing parameters and ratio, as well as size and type of reinforcements. Thus, it is important to select the optimum type and volume fraction of reinforcements and processing parameters. The main aim of this work was to research the influences of volume fractions of reinforcements and FSP parameters on the wear volume loss of 6061-T6 based hybrid composites (AMHCs), and to predict their wear volume loss by using the derived formulation.

1 Experimental

1.1 Materials

In this study, the 6061-T6, pure copper (Cu), 6082, 6630, and 1050-H24 were tagged as 1, 2, 3, 4, and 5, respectively. The chemical compositions of these materials are presented in Table 1.

Table 1 Compositions of experimental materials mass%

Material	Mg	Si	Cu	Zn	Ti	Mn	Cr	C	Pb	Fe	Al
6061-T6	0.85	0.68	0.22	0.07	0.05	0.32	0.06	0	0	0.10	Balance
Copper	0	0	99.90	0.036	0	0	0	0.014	0.005	0	0
6082	0.78	1.06	0.09	0.06	0.01	0.55	0.03	0	0	0.21	Balance
6630	0.31	0.70	0.03	0.06	0.02	0.03	0.01	0	0	0.36	Balance
1050-H24	0.05	0.25	0.05	0.07	0.05	0.05	0.01	0	0	0.4	Balance

1.2 Methods

Fig. 1 shows the schematic view of the FSP tool and grooved plate used in this study. A groove with a given size was acuminated on the plate, and reinforcements were packed into the grooves properly. The different composite structures were manufactured using a hardened tool. It was observed that the tool pin profile, tool rotational and traverse speeds greatly affected the microstructures and mechanical properties of the composites. The used 102 sets of data were divided into training and testing sets. The 84 sets and 18 sets of data, which were selected randomly, were the training and testing data, respectively. The reinforcement volume fractions were calculated by the following equations:

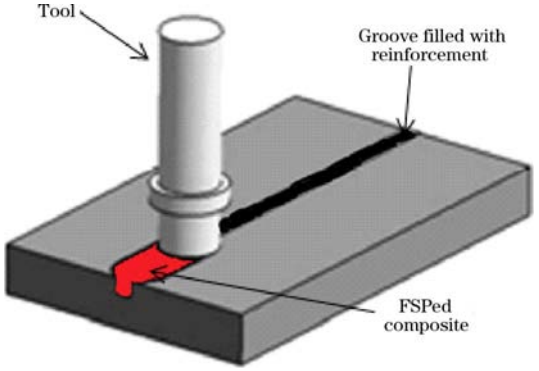

Fig. 1 Schematic illustration of FSP method

$$V_{fr}=\frac{A_g}{A_p}\times 100 \quad (1)$$

$$A_g=W_g\delta_d \quad (2)$$

$$A_p=D_pL_p \quad (3)$$

where, V_{fr} is the reinforcement volume fraction; A_g is the groove area; A_p is the tool pin projected area; W_g is the width of groove; δ_d is the depth of groove; D_p is the diameter of pin, mm; and L_p is the length of pin.

The input data for the matrix were volume fractions of SiC, Gr (graphite), Al_2O_3, TiC and B_4C, size of reinforcement (S, μm); the theoretical volume fraction of reinforcements (V, vol. %), tool rotational speed (r_1, r·min^{-1}), tool traverse speed (r_2, r·min^{-1}), tilt angle (θ), distance from FSP center line of pin (p_1), the number of passes (p_2), sliding distance (s), and load (l). The output variable was wear volume loss. Wear rates (w_r, mm^3) of these composites were estimated by Eq. (4):

$$w_r=\frac{V}{s} \quad (4)$$

The volume fractions and ratios (for instance, SiC/Gr) of reinforcements were estimated separately. All parameters were normalized in the range of 0.05 to 0.95 using Eq. (5):

$$\Phi_{normalized}=a\times\Phi+b \quad (5)$$

where, Φ represents the variables used in the model; and a and b are correspondent and calculated normaliza-

tion coefficients, respectively, as given in Eq. (6):

$$a=\frac{0.90}{i_{\max}-i_{\min}},\ b=0.95-a\cdot i_{\max} \tag{6}$$

where, $i_{\max}$ and $i_{\min}$ are the maximum and minimum values of correspondent variables, respectively.

The influences of volume fractions of reinforcements and processing parameters of FSP on the wear volume loss of the composites can be clearly seen in Table 2. The optimal volume fraction of SiC/Al_2O_3, for example, on the wear volume loss of 1050-H24 alloys which is carried out according to ASTMG190-15 was 50/50 vol. %[29-34].

Table 2 Maximum and minimum values of reinforcements, FSP processing parameters and wear volume loss

Source	Material	SiC/ vol. %	Al_2O_3/ vol. %	Gr/ vol. %	TiC/ vol. %	B_4C/ vol. %	S/ μm	V/ vol. %	d/ mm	r_1/ (r·min^{-1})	r_2/ (r·min^{-1})	θ/ (°)	p_1/ mm	p_2	s/ km	l/ N	w/ mm^3
Ref. [29]	1	66.67	0	33.33	0	0	20	21.43	24	900	40	2.5	1	1	1.00	40	1.39
	1	66.67	0	33.33	0	0	20	21.43	24	1400	40	2.5	1	1	5.00	40	6.32
	1	66.67	33.33	0	0	0	20	21.43	24	900	40	2.5	1	1	1.00	40	2.25
	1	66.67	33.33	0	0	0	20	21.43	24	1 400	40	2.5	1	1	5.00	40	5.40
Ref. [30]	1	0	0	0	0	0	0	0	0	0	0	0	0	0	0.85	40	6.60
	1	66.67	0	33.33	0	0	20	32.14	24	900	40	2.5	2	1	0.85	40	1.81
	1	66.67	0	33.33	0	0	20	32.14	24	900	40	2.5	2	1	7.70	40	22.35
	1	66.67	33.33	0	0	0	20	32.14	24	900	40	2.5	2	1	0.70	40	3.62
	1	66.67	33.33	0	0	0	20	32.14	24	900	40	2.5	2	1	6.50	40	25.36
Ref. [31]	2	0	0	0	0	100	4	11.67	20	800	40	0	0	1	3.00	30	1.57
	2	0	0	0	0	100	4	11.67	20	1200	40	0	0	1	3.00	30	2.33
Ref. [32]	3	0	0	0	0	0	0	0.00	18	1200	60	0	0	1	2.50	25	6.60
	3	0	0	0	100	0	2	24.24	18	1200	60	0	0	1	2.50	25	0.79
Ref. [33]	4	0	0	0	0	0	0	0.00	18	1600	60	0	0	0	2.50	20	2.26
	4	0	0	0	100	0	2	7.90	18	1600	60	0	0	2	2.50	20	0.87
	4	0	0	0	0	100	3	7.90	18	1600	60	0	0	2	2.50	20	1.48
Ref. [34]	5	0	0	0	0	0	0	0	14	1500	100	3	0	3	3.14	2	1.20
	5	100	0	0	0	0	1.25	27.27	14	1500	100	3	0	3	3.14	2	0.35
	5	0	100	0	0	0	1.25	27.27	14	1500	100	3	0	3	3.14	10	3.32

Note: d—Shoulder dimension.

Table 3 gives the maximum and minimum values of the parameters as well as the calculated normalization coefficients. The reinforcements and their properties were also listed in Table 4. It is clearly seen that all the used reinforcements have higher density values compared to aluminum alloys. In order to fix the optimal model architecture, various neuron numbers (14—18) in a hidden layer were used. In order to determine the performance of the model, the correlation coefficient (R) was used, and as error-evaluation

Table 3 Variables used for model and normalization coefficient of input and output parameters

	Variables	Range		Normalization coefficient	
		Maximum	Minimum	a	b
Input	Material code	5.00	1.00	0.225	−0.175
	SiC/vol. %	100.00	0	0.009	0.05
	Al_2O_3/vol. %	100.00	0	0.009	0.05
	Gr/vol. %	33.33	0	0.027 002 7	0.05
	TiC/vol. %	100.00	0	0.009	0.05
	B_4C/vol. %	100.00	0	0.009	0.05
	S/μm	20.00	0	0.045	0.05
	V/vol. %	32.14	0	0.028	0.05
	d/mm	24.00	0	0.037 5	0.05
	r_1/(r·min^{-1})	1600.00	0	0.000 562 5	0.05
	r_2/(r·min^{-1})	100.00	0	0.009	0.05
	θ/(°)	3.00	0	0.3	0.05
	p_1/mm	2.00	0	0.45	0.05
	p_2	3.00	0	0.3	0.05
	s/km	7.70	0.70	0.128 571 429	−0.04
	l/N	40.00	2.00	0.023 684 211	0.002 631 579
Output	w/mm^3	88.20	0.35	0.010 244 735	0.046 414 343

Table 4 Reinforcements and corresponding properties

Reinforcement	SiC	Al_2O_3	Gr	TiC	B_4C
Size/μm	20	20	20	2	4
Density/(g·cm^{-3})	3.166	3.75	2.09	5.21	2.52

criteria, mean absolute percentage error (*MAPE*), mean square error (*MSE*) and mean absolute error (*MAE*) were utilized. *R*, *MAPE*, *MSE* and *MAE* equations have been frequently wielded in other works[35,36].

2 Results and Discussion

2.1 Selection of optimum model structure

Fig. 2(a) shows the macrograph of 5754-H22/CNT surface composite fabricated via FSP method. There are no visable cracks, voids and other defects on the surface of the composites. Fig. 2(b) also reveals the microstructure of 5083/CNT/CeO_2 composite surface taken from the reference[37]. It is clearly seen that the reinforcement materials are homogeneously distributed in the microstructures of the composites.

Table 5 which employs the normalized training and testing data sets, provides statistically the influences of numbers of neuron in. It is clear that the optimum results were obtained with 17 neurons, and 16-17-1 ratio is the optimum model architecture for this research. The *R*, *MAE* and *MSE* values of the training and testing sets for the 16-17-1 model are 0.9995 and 0.9998, 0.002 and 0.005, as well as 0.00002 and 0.00008, respectively. Results shows that the performance of the model is significantly high and reliable[38].

Figs. 3 and 4 illustrate the correlation of experimental and calculated results. According to the test results, it is obvious that R^2 values of the training and testing sets are 0.9988 and 0.9953, respectively. The high R^2 value ($R^2=1$) means that all data spots align completely on the curve, which indicates that the proposed model and test results have excellent correlations and are in good agreement[39].

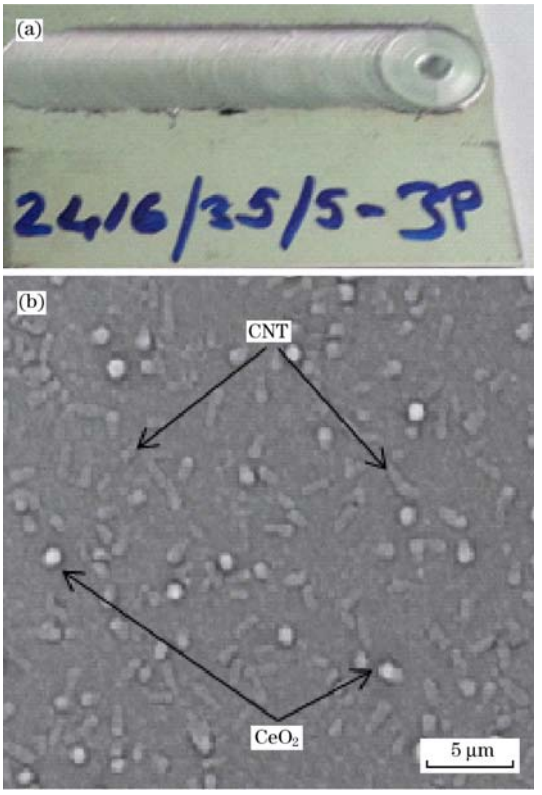

Fig. 2 Macrograph (a) and microstructure (b) of FSP composite

Table 5 Statistical parameters of present model

	Statistical parameter	Neuron number				
		14	15	16	17	18
Training	*MSE*	0.000157313	0.000086017	0.000041008	0.000019775	0.000062868
	R	0.996698264	0.998255586	0.999047457	0.999511687	0.998492048
	MAE	0.006477375	0.004881475	0.003729263	0.002536407	0.005032335
Testing	*MSE*	0.000122685	0.000071367	0.000067026	0.000082264	0.000098040
	R	0.999585960	0.999451346	0.999560063	0.999819908	0.999374151
	MAE	0.006956107	0.006206444	0.005715694	0.005492177	0.006705726

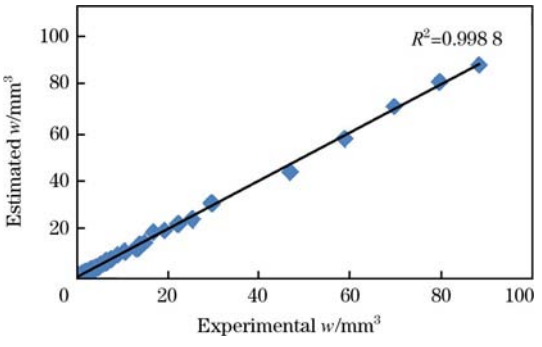

Fig. 3 Correlations of estimated and experimental wear volume loss for training set

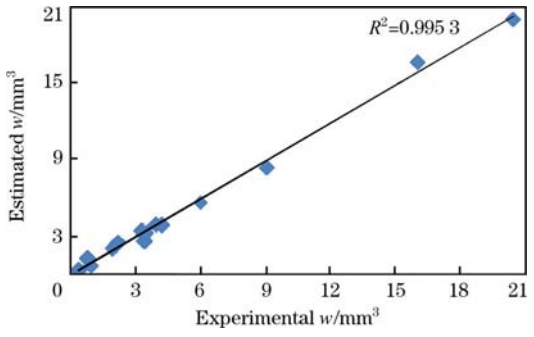

Fig. 4 Correlations of estimated and experimental wear volume loss for testing set

2.2 Formulation of model

The main aim of the work was to study the effects of reinforcement volume fractions and processing parameters of FSP on the wear volume loss (w, mm^3) of 6061-T6 based hybrid composites, and then derive mathematically an equation. Eq. (7) gives the explicit formulation of the wear volume loss as a function of input variables.

$$w=[(1+e^{-z})^{-1}-0.046414343]/0.010244735 \quad (7)$$

where,

$$z=u_1+u_2+u_3+u_4+u_5+u_6+u_7+u_8+u_9+u_{10}+u_{11}+u_{12}+u_{13}+u_{14}+u_{15}+u_{16}+u_{17}-0.20175.$$

The "u" values are:

$$\begin{pmatrix}u_1\\u_2\\u_3\\u_4\\u_5\\u_6\\u_7\\u_8\\u_9\\u_{10}\\u_{11}\\u_{12}\\u_{13}\\u_{14}\\u_{15}\\u_{16}\\u_{17}\end{pmatrix}=\left(\frac{1}{1+e^{-w}}\right)\cdot\begin{pmatrix}1.30\\1.50\\-5.87\\2.71\\1.74\\1.92\\-1.54\\-3.58\\-2.63\\2.41\\0.64\\0.77\\3.22\\0.34\\-0.98\\-0.11\\2.41\end{pmatrix}$$

$$(w_1\ w_2\ w_3\ w_4\ w_5\ w_6\ w_7\ w_8\ w_9\ w_{10}\ w_{11}\ w_{12}\ w_{13}\ w_{14}\ w_{15}\ w_{16}\ w_{17})^{\mathrm{T}}=$$

$$\left(\left(\begin{pmatrix}X_1\\X_2\\X_3\\X_4\\X_5\\X_6\\X_7\\X_8\\X_9\\X_{10}\\X_{11}\\X_{12}\\X_{13}\\X_{14}\\X_{15}\\X_{16}\end{pmatrix}+0.05\right)\cdot\begin{pmatrix}-1.19&-0.21&-0.61&+0.43&-0.07&-1.07&-0.74&-0.75&-0.11&+0.05&+0.59&-0.58&+0.01&-0.60&-0.08&+0.37\\-0.65&-0.21&-0.22&-0.27&+0.46&-0.44&-0.57&-0.87&-0.89&-0.43&+0.02&-1.23&+0.46&-0.13&+1.052&-0.4\\0.76&-0.36&-0.72&+3.7&+0.57&+0.71&+0.37&-0.29&+0.18&+0.50&-0.65&+0.16&-1.09&-0.13&-8.00&+4.13\\-0.26&+0.06&-0.12&-1.80&+0.47&-0.90&-0.52&-0.94&-0.20&-0.82&+0.40&-0.94&-0.44&+0.03&+2.94&+0.25\\-0.51&-0.11&-0.48&-1.22&+0.02&-0.59&-1.25&-0.18&-0.59&-0.93&-0.14&-0.36&+0.09&-0.56&+1.99&-0.16\\-0.53&+0.80&+0.27&-0.07&-0.49&+0.75&+0.01&-0.53&-0.49&+0.04&+1.04&-0.20&+0.01&-0.61&-0.36&+0.93\\-0.52&+0.21&-0.15&+0.60&-0.11&+0.34&+0.10&+1.02&-0.33&-1.65&-0.33&-0.38&+0.19&-0.62&-0.31&-0.73\\1.21&+0.11&+0.42&-0.70&-0.80&-1.15&-0.67&+1.62&-0.19&-0.10&-0.50&-1.00&+1.35&-0.10&-4.41&-2.70\\-0.06&-0.10&-0.71&+1.30&-0.99&+0.10&-1.50&-1.71&+1.77&+0.62&-0.36&+0.66&-2.24&-0.33&-2.24&-1.06\\+0.51&+0.65&+0.07&+1.24&+0.10&+0.38&-0.26&+0.34&+0.14&+0.43&+0.69&+0.09&+1.28&+0.48&-3.39&-0.23\\+0.32&+0.49&+0.02&+0.29&+0.26&-0.33&+0.10&+0.20&+0.55&-0.25&+0.11&-0.23&-0.29&-0.14&-1.10&+0.02\\-0.25&+0.26&+0.50&+0.36&-0.08&+0.34&+0.75&+0.13&+0.82&+0.74&+0.60&+0.14&+1.03&+0.51&+0.19&+0.91\\-1.01&-0.60&+0.12&+2.00&-0.35&-1.09&-2.82&+0.31&-2.24&+1.18&+1.49&-0.23&+0.99&-0.49&+3.83&+0.63\\-0.12&+0.01&+0.41&+0.36&+0.18&+0.50&+0.77&-0.33&+0.57&+0.32&+0.01&+0.59&+0.05&+0.06&-0.97&+0.04\\0.05&+0.22&+0.45&+1.15&-0.19&-0.08&+0.79&+0.16&+0.63&+1.00&+0.08&+0.38&-0.60&+0.71&-1.38&+0.77\\-0.10&-0.46&-0.26&+0.10&+0.03&-0.52&-0.34&-0.16&-0.56&+0.23&-0.17&-0.31&+0.24&-0.17&-0.18&-0.04\\-0.40&+0.11&-0.11&-0.23&+0.38&+0.34&+0.36&-0.47&+0.86&+1.93&+0.96&+0.83&-0.85&+0.48&-2.75&+0.99\end{pmatrix}\right)+\begin{pmatrix}-0.49\\-1.20\\5.01\\-0.74\\-0.66\\0.43\\-0.05\\1.31\\1.02\\-0.33\\-0.02\\-0.69\\-2.37\\-0.14\\1.07\\-0.07\\-0.75\end{pmatrix}$$

where X_1, X_2, X_3, X_4, X_5, X_6, X_7, X_8, X_9, X_{10}, X_{11}, X_{12}, X_{13}, X_{14}, X_{15}, and X_{16} are the normalized input data of material codes, SiC, Al_2O_3, Gr, TiC, B_4C, size of reinforcement, volume fraction of reinforcement, shoulder dimension, tool rotational speed, tool traverse speed, tilt angle, distance from FSP center line of pin, pass number, sliding distance, and load, respectively.

It is important that the proposed formulation is valid for the given ranges in Table 3. The R value and $MAPE$ of the formulation and experimental results (un-normalized results) for the testing sets are 0.999 and 12.84, respectively. The R value demonstrates that the test results are in good agreement with the correlations and produced data. It can be finalized that the wear volume loss of the composites can be calculated with 87.16% accuracy using the proposed equation in this study.

2.3 Parametric studies

The effects of the volume fractions of reinforcements and FSP parameters on the wear volume loss of 6061-T6 hybrid composites were investigated using Eq. (7). Table 6 gives all the experimental results and analysis data obtained under different experimental conditions. Fig. 5 shows the effects of Gr and TiC contents on the wear volume loss of 6061-T6 AMCs. It is clear that the wear volume loss of the composite

Table 6 FSP parameters of 6061-T6 aluminum alloy used in present study

Material	Gr/vol. %	TiC/vol. %	S/μm	V/vol. %	d/mm	r_1/(r·min^{-1})	r_2/(r·min^{-1})	θ/(°)	p_1/mm	p_2	s/km	l/N
6061-T6	0	0	20	5	14	900	40	2.5	0	1	1.00	20

was considerably reduced with the addition of TiC particles. The decrease in volume loss of 6061-T6 AMCs can be attributed to the strengthening mechanisms of work hardening, Orowan strengthening, grain size and shape changes, and quench hardening locally and/or globally in the structure[40]. As can be seen, the dislocations mainly interact with each other and restrict the movement of other dislocations into the composite structures. Thus, dislocation density increases, enhancing the mechanical properties of metals and alloys. Reinforcements are uniformly distributed, so that load can be transferred from the low strength matrix to the strong reinforcement materials, such as CNT, ZrO_2 and TiC. In FSPed metals, grain size refinement was observed, and intermetallics in the microstructure were also splintered and distributed into the matrix due to the FSP process. The high thermal expansion mismatch between the matrix and the reinforcements may cause some changes of the mechanical property as well[41].

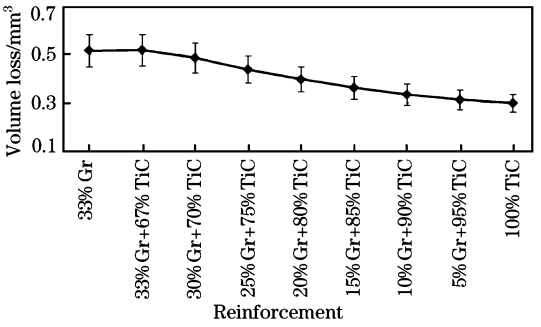

Fig. 5 Effects of Gr and TiC contents on wear volume loss of 6061-T6/Gr/TiC AMHCs

Fig. 6 shows the influences of the volume fractions of 100% TiC, as well as 5% Gr+95% TiC on the wear volume loss of 6061-T6 AMHCs. It was observed that the wear volume loss decreased with increasing volume fractions of the reinforcements. This is probably due to the high hardness of TiC (about 2900 HV) compared to other inclusions. It was previously reported that the hard ceramic particles in the microstructure of Al matrix materials could enhance the hardness and wear resistance of these materials drastically[42,43]. Additionally, the solid lubricant effect plays an important role in improving wear resistance. Note that TiC particles are known to have a solid lubricant effect in various matrix materials[44]. Fig. 7 demonstrates the effect of sliding distance on the wear volume loss of 6061-T6 AMHCs. After analyzing the values in the graphic, it is clear that the amount of wear considerably increased with increasing sliding distance. A maximum sliding distance of wear was about 7.7 km, which is significantly higher than those of other tests.

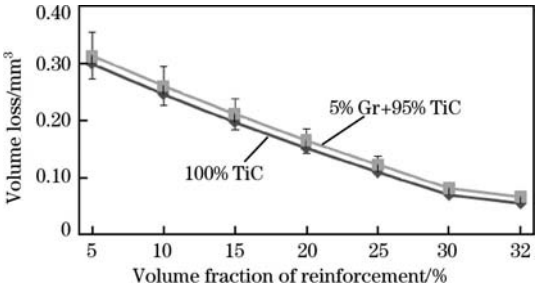

Fig. 6 Effects of volume fractions of reinforcements on wear volume loss of 6061-T6 AMHCs

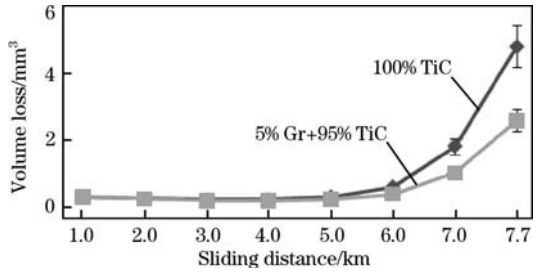

Fig. 7 Effects of sliding distance on wear volume loss of 6061-T6 AMHCs

Figs. 8 and 9 illustrate the effects of tool traverse and rotational speeds on the wear volume loss of 6061-T6 AMHCs, respectively. It was observed that an increase in the tool rotational speed enhanced the wear volume loss. This can be due to the softening of the matrix and more surface interactions with increasing rotational speeds. It is known that increasing the rotational speed increases the heat generation, hereby, the produced high heat induces matrix softening, which results in reduced wear resistance of aluminum matrix composites[45]. The wear volume loss was also confirmed to rise with increasing tool traverse speeds. The homogeneous distribution of particles, impurities, voids, surface oxidations, cracks, as well as high and low heat inputs during

friction stir processing can mainly affect the mechanical and wear properties of composites[46-48]. Decrease in the wear volume loss with increasing tool traverse speed can be due to the lower heat generation. It was stated that the average grain size of composites produced by the FSP method may adversely affect the mechanical properties of the substrates[33]. The lower wear volume loss was gotten under the optimal condition of tool rotational and traverse speeds of 900 r/min and 40 mm/min, respectively.

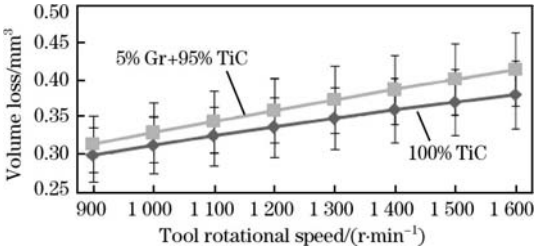

Fig. 8 Effects of tool rotational speed on wear volume loss of 6061-T6 AMHCs

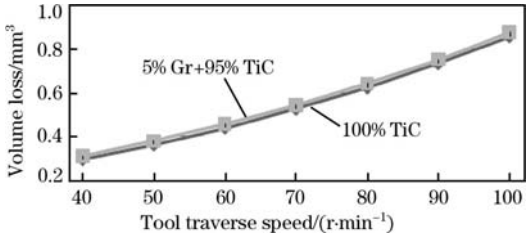

Fig. 9 Effects of tool traverse speed on wear volume loss of 6061-T6 AMHCs

Fig. 10 shows the influences of complex reinforcements on the volume loss of 6061-T6 AMCs. The following ratios of 50% SiC + 50% TiC, 50% SiC + 25% TiC + 25% Al_2O_3, 50% SiC + 50% Al_2O_3, 25% SiC + 50% TiC + 25% Al_2O_3, 25% SiC + 25% TiC + 50% Al_2O_3, and 50% TiC + 50% Al_2O_3 were labeled as A, B, C, D, E, and F, respectively. These inclusions were all hard and brittle for wear applications. The results demonstrated that the wear volume loss of the 6061-T6 hybrid composite with 50% TiC + 50% Al_2O_3 was significantly lower than those of the other composites. This might be due to the solid lubricant effects of TiC and Al_2O_3, i. e., high hardness of TiC, as well as the load supporting effect of Al_2O_3[34]. The Al_2O_3 particles avoided direct metal-to-metal contact and served as a solid lubricant or rolling objects. As stated earlier, TiC particles could also act as a solid lubricant. These effects substantially reduced the coefficient values of friction and increased the wear resistance of the Al matrix composites. The bond strength at interface of the matrix and reinforcement, type and homogeneous distribution of reinforcements, surface morphologies and oxidations, as well as the processing parameters of FSP influence the wear resistance of composites fabricated by FSP technique[36]. It is very difficult to detect the influences of all factors on the wear volume loss of the composites, so detailed works are required to mention these hypotheses.

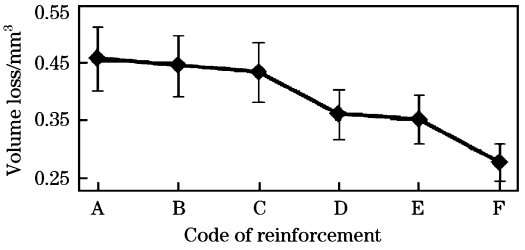

Fig. 10 Effects of complex reinforcements on wear volume loss of 6061-T6/SiC/TiC/Al_2O_3 AMHCs

3 Conclusion

The wear resistances of 6061-T6 based composites decreased with increasing the traverse and rotational speeds of tool. The optimum complex reinforcement volume fractions in 6061-T6 based AMHCs were determined using the 50% TiC + 50% Al_2O_3 inclusions for better wear resistance. The designed and analyzed explicit formulation of 16-17-1 ratio which was the optimal model architecture was studied, and the testing phase results provided that the proposed formulation exhibited a high reliability where all R and R^2 values are larger than 0.99 and can be used generalizing the relationship between input and output parameters. The results also demonstrated that the wear volume loss of the hybrid composites was calculated with an accuracy of 87.16% with the derived formulation.

References:

[1] D. Das, P. Mishra, S. Singh, S. Pattanaik, Int. J. Mech. Mater. Eng. 9 (2014) 1-15.
[2] C. M. L. Wu, G. W. Han, Mater. Charact. 58 (2007) 416-422.
[3] S. P. Rawal, JOM 53 (2001) 14-17.
[4] J. Hooker, P. Doorbar, Mater. Sci. Technol. 16 (2000) 725-731.
[5] C. Leyens, M. Peters, Titanium and Titanium Alloys, Wiley Online Library, 2003.
[6] A. Macke, B. F. Schultz, P. Rohatgi, Adv. Mater. Processes 170 (2012) 19-23.
[7] T. V. Christy, N. Murugan, S. Kumar, J. Min. Mater. Charact. Eng. 9 (2010) 57-65.
[8] D. Lu, Y. Jiang, R. Zhou, Wear 305 (2013) 286-290.
[9] K. M. Shorowordi, A. S. M. A. Haseeb, J. P. Celis, Wear 261 (2006) 634-641.

[10] N. Murugan, B. Ashok Kumar, Mater. Des. 51 (2013) 998-1007.
[11] N. Yuvaraj, S. Aravindan, J. Mater. Res. Technol. 4 (2015) 398-410.
[12] X. Tong, Thermally Conductive Ceramic Matrix Composites, Advanced Materials for Thermal Management of Electronic Packaging, Springer, New York, 2011, pp. 277-304.
[13] S. R. Anvari, F. Karimzadeh, M. H. Enayati, Wear 304 (2013) 144-151.
[14] K. Funatani, K. Kurosawa, Adv. Mater. Processes 146 (1994) 27-30.
[15] M. Skibo, P. Morris, D. Lloyd, Proceedings of the World Materials Congress, Chicago, 1988, pp. 257-262.
[16] D. Huda, M. E. Baradie, M. Hashmi, J. Mater. Process. Technol. 37 (1993) 513-528.
[17] D. C. Hofmann, K. S. Vecchio, Mater. Sci. Eng. A 402 (2005) 234-241.
[18] A. Dolatkhah, P. Golbabaei, M. K. Besharati Givi, F. Molaiekiya, Mater. Des. 37 (2012) 458-464.
[19] M. Raaft, T. S. Mahmoud, H. M. Zakaria, T. A. Khalifa, Mater. Sci. Eng. A 528 (2011) 5741-5746.
[20] H. I. Kurt, Composites Part B: Engineering 93 (2016) 26-34.
[21] R. Nandan, T. DebRoy, H. K. D. H. Bhadeshia, Progress in Materials Science 53 (2008) 980-1023.
[22] Y. Morisada, H. Fujii, T. Nagaoka, M. Fukusumi, Mater. Sci. Eng. A 419 (2006) 344-348.
[23] E. R. I. Mahmoud, M. Takahashi, T. Shibayanagi, K. Ikeuchi, Sci. Technol. Weld. Join. 14 (2009) 413-425.
[24] S. J. Vijay, N. Murugan, Mater. Des. 31 (2010) 3585-3589.
[25] R. Ashok Kumar, M. Thansekhar, Advanced Materials Research, Trans. Tech. Publ. 2014, pp. 586-591.
[26] S. M. Aktarer, D. M. Sekban, O. Saray, T. Kucukomeroglu, Z. Y. Ma, G. Purcek, Mater. Sci. Eng. A 636 (2015) 311-319.
[27] Z. Y. Ma, S. R. Sharma, R. S. Mishra, Scripta Mater. 54 (2006) 1623-1626.
[28] Y. Bozkurt, H. Uzun, S. Salman, J. Compos. Mater. 45 (2011) 2237-2245.
[29] D. Aruri, K. Adepu, K. Adepu, K. Bazavada, J. Mater. Res. Technol. 2 (2013) 362-369.
[30] A. Devaraju, A. Kumar, B. Kotiveerachari, Trans. Nonferrous Met. Soc. China 23 (2013) 1275-1280.
[31] R. Sathiskumar, I. Dinaharan, N. Murugan, S. J. Vijay, Trans. Nonferrous Met. Soc. China 25 (2015) 95-102.
[32] A. Thangarasu, N. Murugan, I. Dinaharan, S. J. Vijay, Archives of Civil and Mechanical Engineering 15 (2015) 324-334.
[33] C. M. Rejil, I. Dinaharan, S. J. Vijay, N. Murugan, Mater. Sci. Eng. A 552 (2012) 336-344.
[34] E. R. I. Mahmoud, M. Takahashi, T. Shibayanagi, K. Ikeuchi, Wear 268 (2010) 1111-1121.
[35] H. I. Kurt, M. Oduncuoglu, Mathematical Problems in Engineering 2015 (2015) 710526.
[36] H. I. Kurt, M. Oduncuoglu, Int. J. Polym. Sci. 2015 (2015) 315710.
[37] S. A. Hosseini, K. Ranjbar, R. Dehmolaei, A. R. Amirani, J. Alloys Comp. 622 (2015) 725-733.
[38] H. Kurt, M. Oduncuoglu, Metals 5 (2015) 371-382.
[39] H. Kurt, M. Oduncuoglu, M. Kurt, Metals 5 (2015) 836-849.
[40] D. J. Lloyd, Int. Mater. Rev. 39 (1994) 1-23.
[41] A. C. Lund, C. A. Schuh, Mechanical Properties: Strengthening Mechanisms in Metals A2-Wyder, Franco BassaniGerald L. LiedlPeter, Encyclopedia of Condensed Matter Physics, Elsevier, Oxford, 2005, pp. 306-311.
[42] A. P. Semenov, J. Frict. Wear 28 (2007) 401-408.
[43] A. Siddharth Sharma, K. Biswas, B. Basu, Wear 319 (2014) 160-171.
[44] T. Mang, W. Dresel, Lubricants and Lubrication, 2nd ed., Wiley, Germany, 2007.
[45] A. Shafiei-Zarghani, S. F. Kashani-Bozorg, A. Zarei-Hanzaki, Mater. Sci. Eng. A 500 (2009) 84-91.
[46] R. V. Barenji, Proceedings of the Institution of Mechanical Engineers, Part L: Journal of Materials Design and Applications, 2015: 1464420715584950.
[47] C. Sharma, D. K. Dwivedi, P. Kumar, Mater. Des. 36 (2012) 379-390.
[48] A. V. Kolubaev, E. A. Kolubaev, O. V. Sizova, A. A. Zaikina, V. E. Rubtsov, S. Y. Tarasov, P. A. Vasiliev, J. Frict. Wear 36 (2015) 127-131.